Materials Chemistry and Physics 112 (2008) 504–509

Contents lists available at ScienceDirect

Materials Chemistry and Physics

journal homepage: www.elsevier.com/locate/matchemphys

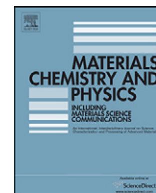

Hardness of zirconium diboride films deposited on titanium substrates

J.V. Rau [a,*], D. Ferro [b], M.B. Falcone [c], A. Generosi [a], V. Rossi Albertini [a], A. Latini [c], R. Teghil [d], S.M. Barinov [e]

[a] *Istituto di Struttura della Materia, CNR, via del Fosso del Cavaliere 100, 00133 Rome, Italy*
[b] *Istituto per lo Studio dei Materiali Nanostrutturati, CNR, Piazzale Aldo Moro 5, 00185 Rome, Italy*
[c] *SAPIENZA Universitá di Roma, Dipartimento di Chimica, Piazzale Aldo Moro 5, 00185 Rome, Italy*
[d] *Universitá della Basilicata, Dipartimento di Chimica, via N. Sauro 85, 85100 Potenza, Italy*
[e] *Baikov Institute of Metallurgy and Materials Science, Russian Academy of Sciences, Leninskij Prospect 49, Moscow 119991, Russia*

ARTICLE INFO

Article history:
Received 3 April 2008
Received in revised form 23 May 2008
Accepted 4 June 2008

Keywords:
Thin films
Pulsed laser deposition
Electron beam deposition
Hardness

ABSTRACT

The study was aimed at the hardness determination of thin ZrB_2 films produced on pure titanium substrate by pulsed laser deposition and electron beam deposition techniques. The former method allows the deposition of dense crystalline films, being textured preferentially along the (1 1 0) direction, whereas the electron beam deposition allows the production of compact X-ray amorphous films. The thickness of the films was about 200 and 500 nm, respectively. Vickers hardness values obtained by microindentation technique are close to those of bulk ZrB_2 ceramics. Pulsed laser deposited ZrB_2 films are harder ranging from 21 to 27 GPa than the electron beam deposited films ranging from 19 to 23 GPa. An increase in the substrate preheating temperature leads to a decrease in hardness value.

© 2008 Elsevier B.V. All rights reserved.

1. Introduction

Refractory zirconium diboride (ZrB_2) possesses several excellent properties which makes it a promising coating material for various industrial applications, such as, for example, semiconductors technology (as diffusion barriers on silicon) and nuclear technology (boron-containing compounds used as neutron adsorbers) [1]. Among these properties, the following can be mentioned: high melting point (about 3300 K) [2], high bulk hardness (22 GPa) [3], good corrosion resistance, low friction coefficient and low bulk resistivity [4].

In the literature, ZrB_2 films deposited on several substrates, such as Al_2O_3, SiC, Si(1 1 1) [5]; Si(0 0 1) [6]; steel, aluminium [7]; quartz, zircaloy-4 [8,9], are reported. In this study, we examine zirconium diboride films deposited on titanium substrates. Titanium is light material, relatively soft (bulk hardness about 2 GPa) and exhibits a low wear resistance. Therefore, a protective coating of the titanium surface might improve its characteristics and performances. In particular, a ZrB_2 coating could provide protection against oxidation of titanium, enhance its hardness and its corrosion and wear resistance.

Two methods were used in our study to produce ZrB_2 film on Ti substrates, namely pulsed laser deposition (PLD) and electron beam deposition (EBD). Each coating process has inherent advantages and disadvantages affecting the coating properties. For example PLD, on one side, usually provides strong bonding between film and substrate; on the other side, allows to deposit very thin films, to control surface roughness, to ablate any material and to fabricate coatings on any substrate material, e.g. metal, ceramic and plastic. Unfortunately, PLD still remains expensive and, at present, is not yet adopted for coating of the large surfaces, thus hampering its application in industry. The EBD method is more versatile, although preheating of substrate is needed to reach satisfactory adhesion strength of the film to the substrate.

The present work is aimed at determining the Vickers hardness of ZrB_2 films deposited by PLD and EBD on Ti substrates. To further characterize the films, the Scanning Electron Microscopy (SEM) coupled with a system for microanalysis (energy dispersive X-ray spectroscopy, EDXS), and X-ray diffraction (both in the angular (AXRD) and in the energy dispersive (EDXD) modes) were employed.

2. Experimental

2.1. Film deposition techniques

Targets for deposition were fabricated from a ZrB_2 powder (95% pure; Aldrich Chemical Co.), hot pressed into pellets. The titanium substrates were sandblasted prior to deposition by a 60-grid SiC abrasive, in order to increase their surface roughness, R_a, up to approximately 1.6 nm.

2.1.1. Pulsed laser deposition

The PLD apparatus for film deposition has been described in detail elsewhere [10]. It consists of a vacuum chamber equipped with a rotating support for the target,

* Corresponding author. Tel.: +39 06 4991 3641; fax: +39 06 4991 3951.
E-mail address: giulietta.rau@uniroma1.it (J.V. Rau).

0254-0584/$ – see front matter © 2008 Elsevier B.V. All rights reserved.
doi:10.1016/j.matchemphys.2008.06.004

quartz windows for the inlet of the laser beam and a substrate holder. The ablation laser source was a frequency-doubled Nd:glass laser (527 nm emission wavelength, 250 fs pulse duration, E = 2.3 mJ, 10 Hz repetition rate). The laser beam was inclined at 45° with respect to the ZrB_2 target surface and in-axis with the Ti substrate, placed at a distance of 2 cm from the target. The deposition time was 2 h and the films were deposited at two different substrate preheating temperatures (T_{sp} = 300 and 500 °C). All the experiments were carried out in high vacuum (4×10^{-4} Pa).

2.1.2. Electron beam deposition

The ZrB_2 target to be evaporated was placed into a crucible made of titanium diboride/boron nitride composite (GE Advanced Ceramics, UK). The crucible was then inserted into a water-cooled electron beam gun (EVI-8, Ferrotec, Germany), which is positioned into a stainless-steel chamber evacuated by a turbomolecular pump supported by a rotative pump. The distance between the target and the substrate was set at 25 cm. The accelerating voltage (in the range [−10, −3.05] kV), the shape, pattern and position of the beam were controlled. The maximum operation power was set at 5 kW. The gun has a magnetic lens system that allows a 270° deflection of the beam to prevent contamination of the ablated material with tungsten vapours emitted by the cathode filament. Before and during the deposition process, the substrates were heated under vacuum of 5×10^{-3} Pa in the chamber by a high-power halogen lamp, their temperature being measured by a K-type thermocouple. The deposition process was performed at an EB accelerating voltage −5 kV and at an emission current of 130–200 mA. The cross section of the electron beam was circular and the electrons speed low, to ensure uniform consumption of the evaporating material. Under these conditions, the deposition rate was 1–5 Å s^{-1}. The evaporation process is quite problematic due to the severe spitting of the target. The coated samples were cooled to room temperature in a nitrogen atmosphere before removal from the chamber.

The thickness of the growing films, as well as the deposition rates, was real-time monitored by a quartz microbalance. The microbalance is based on the acoustic impedance of the deposited material, which is the product between the acoustic velocity of sound in the material and the material density. For a given material, the acoustic velocity of sound is given by the formula:

$$V = \sqrt{\frac{\mathrm{BM}}{\rho}} \quad (1)$$

where BM is the bulk modulus of elasticity of the material and ρ is the density. The microbalance controller needs to be calibrated by measuring the so-called "z factor", which is given by the ratio between the acoustic impedance of quartz and the acoustic impedance of the deposited material. The thicknesses of the two ZrB_2 films, deposited on the preheating Ti substrate (T_{sp} = 350 and 500 °C), were estimated by the microbalance method and resulted to be about 0.5 μm.

2.2. Scanning electron microscopy (SEM) morphological analysis

Scanning electron microscopy (SEM) carried out with a LEO 1450 variable pressure apparatus, with a tungsten emitter and resolution of 4 nm, was used to observe in secondary electron mode the morphology of the ZrB_2 films. The SEM apparatus is coupled with a system for microanalysis EDXS INCA 300. The atomic number contrast presented on the SEM images as grey colour hues can be observed thanks to the ability of the Everhart Thornley detector to collect a part of the backscattered electrons, because of the favourable geometry of sample and detector. This approach has been adopted for the film thickness measurements, since it permits to precisely distinguish the film boundary. To confirm the results of the atomic number contrast, the EDXS analysis of the chemical nature of the observed phase has been carried out. The thickness of both PL-deposited ZrB_2 films (T_{sp} = 300 and 500 °C) was estimated to be about 0.20 ± 0.04 μm.

2.3. X-ray diffraction

2.3.1. Angular X-ray diffraction mode (AXRD)

Conventional angular X-ray diffraction measurements were performed by a Philips X'Pert PRO diffractometer (Cu Kα_1 radiation, λ = 1.54056 Å) equipped with two gas filled proportional detectors, one for powders and the other for thin films. The thin film detector is coupled with a graphite monochromator to enhance the signal to noise ratio by removing the incoherent contributions from the scattered beam.

2.3.2. Energy dispersive X-ray diffraction mode (EDXD)

The general principles of the energy dispersive X-ray diffraction method have been described elsewhere [11]. EDXD measurements were performed to obtain information about the crystalline structure, the texture and grain size only for two (of the four reported) ZrB_2 film samples: the PL-deposited ZrB_2 films. In case of the EB- deposited ZrB_2 films, regardless the T_{sp} (350 or 500 °C), no crystalline signal arising from the film was detected, despite rather long acquisition time (12 h).

A static data collection was carried out in the reflection geometry (ϑ–ϑ configuration, ϑ being half the scattering angle), at an inclination angle of the sample with respect to the primary beam corresponding to the maximum intensity of the X-rays diffracted by the Ti substrate (top of the substrate rocking curve).

Indeed, in the energy dispersive mode, the whole diffraction pattern is collected simultaneously at any value of the scattering parameter $q = KE \sin\vartheta$ (where K is a constant equal to 1.014 $Å^{-1}$ keV^{-1} and E is the photon energy in keV) by making use of a polychromatic primary beam. No mechanical movement is required during the measurement because, in this case, the scan of the reciprocal space is performed electronically by an energy sensitive solid state Ge detector (15–55 keV), while the diffraction angle is kept unchanged.

To reduce the signal to noise ratio, the overall diffracted intensity was acquired for 8 h.

The experimental conditions – maximum photon energy 55 keV, diffraction angle ϑ = 6.3° – were chosen to obtain a diffraction pattern in the q-range (1.50, 5.50)$Å^{-1}$, which contains all the main Bragg reflections of the ZrB_2 powder and corresponds to the d-range (1.14, 4.20) Å.

2.4. Vickers hardness measurements

Hardness of the composite film/substrate system was measured by means of a Leica VMHT apparatus (Leica GmbH, Germany) equipped with a standard Vickers pyramidal indenter (square-based diamond pyramid of face angle 136°) according to the procedure described in detail in our previous works [12,13]. The loading and unloading speed was 5×10^{-6} m s^{-1} and the time under the peak load was 15 s. Indentations were made with 5 loads ranging from 0.1 to 19.6 N. To express the hardness, H_c, of the film/substrate system as a function of its components, film (H_f) and substrate (H_s), a Jönsson and Hogmark model based on an area law-of-mixture approach was used [14], taking into account also the indentation size effect [15,16]. A reasonable expression for the H_c in this case is

$$H_c = H_{s0} + \frac{B_s + 2ct(H_{f0} - H_{s0})}{D} \quad (2)$$

where $c \cong 0.5$ for a brittle hard film on a more ductile substrate [14]; H_{s0} and H_{f0} are the intrinsic hardness of substrate and film, respectively; t is the film thickness; D is the imprint diagonal, and B_s is the coefficient, which was determined in a separate experiment on the hardness of the Ti substrate. To calculate the intrinsic hardness of the film, special attention was paid to correctly choose the indentation depths, d, i.e. in the interval where the model is adequate. According to the estimations, the d/t ratio must be in the range from 2 to approximately 20, providing substrate-dominated mixed region where the film is fractured conforming to the plastically deforming substrate [17]. In this range of d/t, the results obtained by using the Jönsson and Hogmark model has been demonstrated to coincide well with those resulting from more complicated approaches (Korsunsky et al., Chicot–Lessage) [18].

3. Results and discussion

SEM micrographs of PL- and EB-deposited ZrB_2 films are shown on Figs. 1 and 2. Fig. 1(a) shows the PL-deposited ZrB_2 film on Ti substrate (T_{sp} = 300 °C) at low magnification. The film surface appears to be continuous and uniform, reproducing the substrate roughness. At a higher magnification (Fig. 1(b)) a dense grain texture is revealed. The grain size distribution appears to be bilobate, rather than uniform or Gaussian. The grains can therefore be divided into two groups: a group with approximately 40–50 nm grain diameter and another one with a much larger grain size 200–250 nm. On Fig. 1(c), the PL-deposited ZrB_2 film on Ti substrate (T_{sp} = 500 °C) is shown at high magnification and a similar grain texture is observed. Also in this case, two groups could be distinguished: a group of 30–50 nm grain diameter and another one of 250–350 nm grain diameter.

The surface of the EB-deposited ZrB_2 films is smooth and compact. On Fig. 2(a), the ZrB_2 film surface (T_{sp} = 350 °C) is present appearing as a not perfectly continuous layer. At higher temperature (T_{sp} = 500 °C) (Fig. 2(b)) the surface morphology improves, so that the SEM observations taken at higher magnification do not reveal any discontinuity.

According to the SEM-EDXS data analysis, the Zr/B atomic ratio in the films is close to the ZrB_2 stoichiometric ratio, being 1:2 for PL-deposited films and 1:1.8 for EB ones. In the latter samples, the presence of small amounts of oxygen was also detected.

As estimated by SEM cross-sectional observation, the thickness of the PL-deposited films is 0.20 ± 0.04 μm, while the thickness of the EB-deposited ones is 0.50 ± 0.10 μm. This estimation fits well the microbalance data.

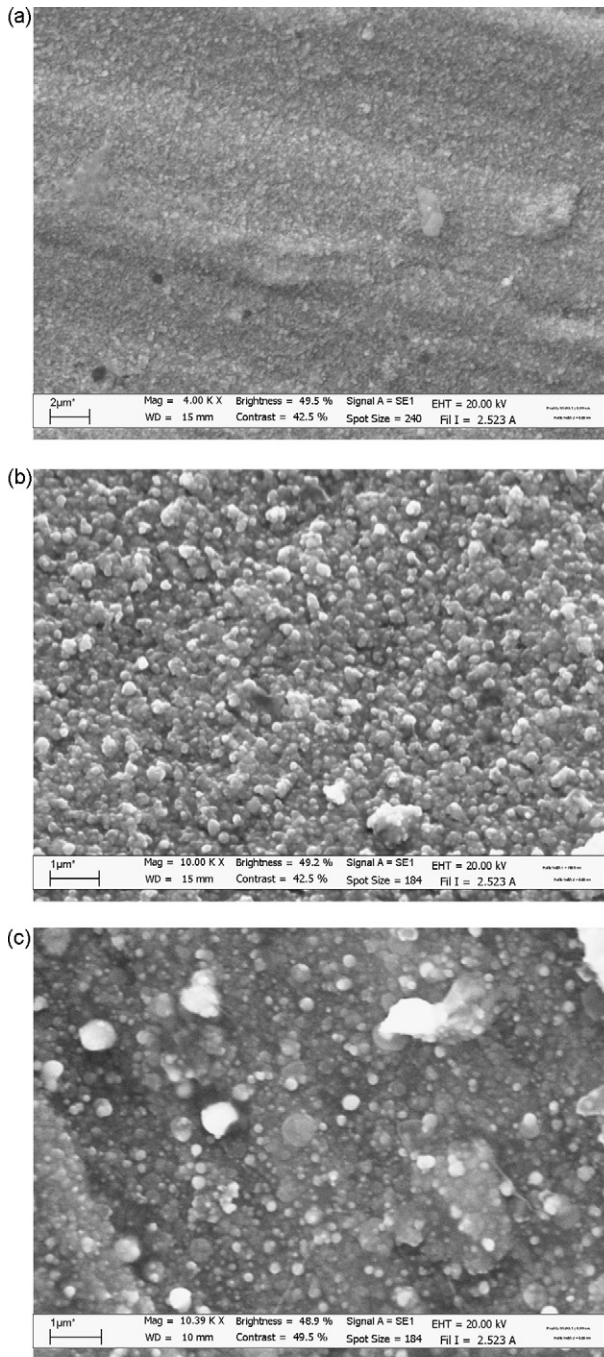

Fig. 1. SEM micrographs of PL-deposited ZrB_2 films on Ti substrate: (a and b) T_{sp} = 300 °C and (c) T_{sp} = 500 °C.

Preliminary conventional AXRD measurements were performed to characterize the ZrB_2 target prior to deposition, and its pattern is presented in Fig. 3. All ZrB_2 crystalline peaks are visible, their orientation and angular position being labelled in figure (JCPDS database, ZrB_2 card 75-0964), proving the target has no privileged orientation.

Afterwards, X-ray diffraction data were collected in the ED mode to characterize both the EB-deposited and the PL-deposited ZrB_2 films. The first proved to be X-ray amorphous with a small crystalline admixture of ZrO. The presence of oxygen was also confirmed by the SEM-EDXS analysis.

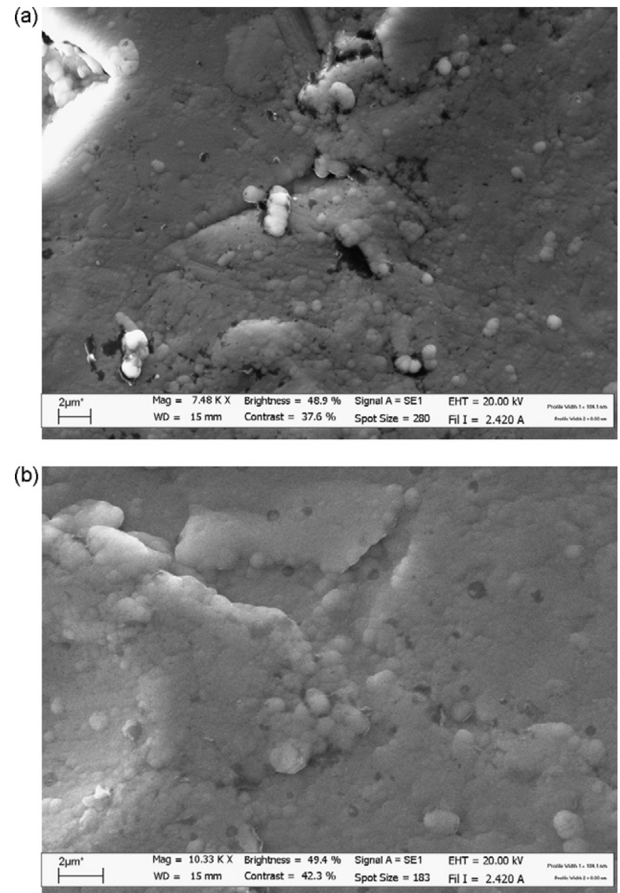

Fig. 2. SEM micrographs of EB-deposited ZrB_2 films on Ti substrate: (a) T_{sp} = 350 °C and (b) T_{sp} = 500 °C.

The EDXD diffraction patterns of the PL-deposited ZrB_2 films are shown in Fig. 4(a and b). As it can be seen, all the substrate reflections were detected and labelled according to the literature data (Ti has hexagonal lattice, space group $P6_3/mmc$), and an intense (1 1 0) direction growth (17% relative intensity according to the literature powder diffraction data) was found for both the ZrB_2 films. Indeed, despite the very long acquisition times and the capability of the ED mode to reduce the noise to signal ratio significantly (since the whole pattern is collected simultaneously), only minimal traces of the (1 0 0) reflection signal could be found in the film deposited at 300 °C. Such reflection, associated to a 76% relative intensity according to the literature powder diffraction data, is evidenced in Fig. 4(a)

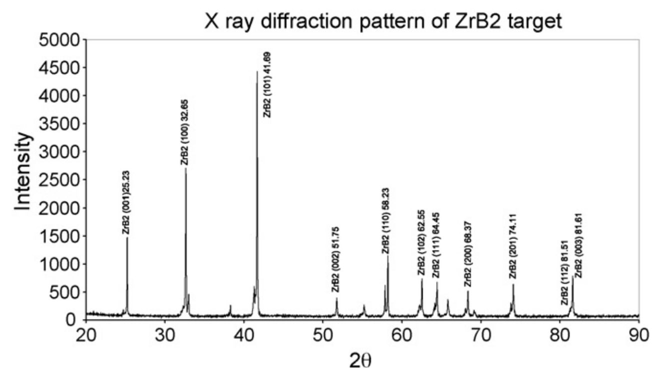

Fig. 3. AXRD pattern of the ZrB_2 target.

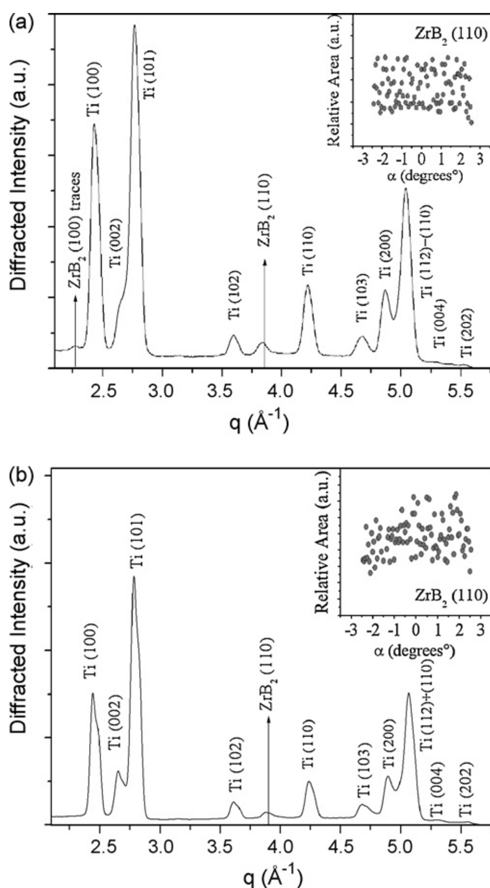

Fig. 4. EDXD patterns of PL-deposited ZrB_2 film on Ti substrate: (a) T_{sp} = 300 °C and (b) T_{sp} = 500 °C. In the insets, the rocking curve of the ZrB_2 (1 1 0) reflection is shown.

by an arrow. Moreover, the most intense powder diffraction signal (1 0 1) at q = 2.90 Å is missing.

In the film grown at 500 °C, no traces of other crystalline growth directions were detected in as much as 8 h of acquisition time.

These considerations support the hypothesis of preferential growth of the ZrB_2 film along the (1 1 0) direction for both samples. In order to confirm whether the (1 1 0) direction is truly the preferential growth direction or if the films may be a polycrystal characterized by a spread mosaic texture, a rocking curve (RC) analysis was performed. Indeed, the RC of a polycrystal represents the statistical distribution of the crystallites orientation. In EDXD, it can be obtained normalizing the intensity of a given Bragg peak, collected as a function of an asymmetry parameter $\alpha = (\vartheta_i - \vartheta_r)/2$, (where ϑ_i, ϑ_r are the incident and reflection angles, respectively, while the total scattering angle $(\vartheta_i + \vartheta_r) = 2\vartheta$ is kept unchanged), to its maximum intensity observed along the α scan. Moreover, when the RC measurements are performed, the EDXD mode is particularly efficient, since all Bragg peaks present in the selected q-region are collected simultaneously. This allows the calculation of the RC of all the visible reflections, providing a richer statistical information on the sample structure.

The PL-deposited ZrB_2 film samples where placed upon a rocking cradle in the optical centre of the ED diffractometer and the RC measurements were performed in the asymmetry range ($-2.5^\circ < \alpha < 2.5^\circ$), wide enough to reveal whether the film can be regarded as a polycrystal or as an assembly of powder-like independent domains. The rocking steps were set at $\Delta\alpha = 0.1^\circ$.

In the selected asymmetry range, no other ZrB_2 Bragg reflections were detected besides the (1 1 0) one, confirming the hypothesis of a privileged growth direction for the individual crystallites. The RC data analysis was then executed for this reflection and the results are shown in the insets of Fig. 4(a and b). The intensity distribution of the peak (deduced by its Gaussian fit) as a function of α is flat, with steady random fluctuations only, thus suggesting that the (1 1 0)-grown crystallites have random orientations with respect to the substrate surface.

The crystallites average size was calculated by using the Laue equations to obtain an expression for the EDXD mode, equivalent to the Scherrer formula which is valid for the AXRD mode only: $(1/2)tq_1 = (n-1)\pi$ and $(1/2)tq_2 = (n+1)\pi$; where t is the crystallites average diameter; q_1 and q_2 are the interference function zeros adjacent to the function maximum ($q_1 < q_2$); n is the order of the interference function peaks (the parameter that labels the features of the "sinc" interference function) [19].

Combining these two equations, the grain size t is obtained, $t = 4\pi/(q_2 - q_1)$. In the Scherrer approximation (triangular shape of the interference peak) $t \cong 2\pi/\sigma_{(hkl)}$, where $\sigma_{(hkl)}$ is the standard deviation of the (hkl) peak intensity distribution due to the crystallite finite size.

This expression of the finite size effect can be used to estimate the average diameter of the crystallite from the overall standard deviation of the Bragg peak. Indeed, such overall standard deviation σ^2 can be written as $\sigma^2 = \sigma_r^2 + \sigma_{(hkl)}^2$, where σ_r^2 represents the contribution to the peak broadening due to the instrumental resolution (both angular and energy spreads), which can be measured independently.

From this analysis, the average size of the (1 1 0) crystallites resulted to be (40 ± 5) nm for the PL-deposited ZrB_2 film (T_{sp} = 300 °C) and (25 ± 5) nm for that of (T_{sp} = 500 °C). These results are in agreement with the SEM data discussed above. Indeed, for the PL-deposited ZrB_2 film sample (T_{sp} = 300 °C), the minimum grain size reported is 40–50 nm and for the PL-deposited ZrB_2 film sample (T_{sp} = 500 °C) is 30–50 nm. Such small grains dominate the peaks shape, because the presence of some bigger crystallites (visible in the SEM image) does not significantly balance the Bragg reflections broadening induced by the finite size effect.

It should be noted that the EDXD and SEM results on the grain size are consistent, although the former estimates the grains size value averaged on the whole sample, while the latter is a local measurement. The agreement confirms the uniformity and homogeneity of the deposition, in the sense that the local values of the morphological parameters correspond to the general values, as well as the reliability of the joint use of the techniques.

In Fig. 5(a and b) the experimental plots composite hardness (H_c) versus inverse imprint diagonal ($1/D$) for all four deposited samples are presented. The plots were well approximated by a linear regression. Calculated intrinsic hardness values for ZrB_2 films under study are given in Table 1. The bulk hardness of zirconium diboride ceramics is 22 GPa according to [7] and ranges from 18 to 30 GPa according to [20]. As can be seen from Table 1, all hardness values fall in a range close to that of bulk ceramics. For comparison, the Vickers hardness of the ZrB_2 coating on the steel substrate was reported to be 19.3 ± 2.1 GPa [7].

Comparing the results obtained for PL- and EB-deposited ZrB_2 film samples, one can see that, at the same substrate preheating temperature, PL-deposited films are harder. This is likely due to their dense grain nature. EB-deposited films are X-ray amorphous and less hard. The substrate preheating temperature is another factor influencing the film hardness. A temperature increase to 500 °C leads to a decrease in the hardness value of about 22% for PL-deposited samples (from 27 to 21 GPa, respectively) and of about 17% for EB-deposited ones (from 23 to 19 GPa, respectively) (see Table 1).

Table 1
Hardness of ZrB_2 films on Ti substrate

Deposition method	Substrate preheating temperature (°C)	Film thickness (μm)	Film hardness (Vickers, GPa)
PLD	300	0.2	27 ± 4
PLD	500	0.2	21 ± 3
EBD	350	0.5	23 ± 3
EBD	500	0.5	19 ± 3

In our previous studies, we observed a similar temperature effect for TiC films on Ti substrate [12]. Also in that case, the higher substrate preheating temperature resulted in a decrease in hardness, due to the diffusion of carbon from the TiC film into the Ti substrate. In the present case, it should however be noted that no traces of TiB_2 peaks are present on the ZrB_2 film diffraction patterns. Besides, no peaks related to intermediate phases, such as either $Zr_{0.8}Ti_{0.2}B_2$ or $Ti_{0.8}Zr_{0.2}B_2$ phases [21], were detected, and no shift of ZrB_2 peaks was observed. These entire findings lead to the opinion that there is no diffusion of boron from the film into the substrate and, consequently, that no interaction between the ZrB_2 film, once formed, and Ti substrate took place, since zirconium diboride is extremely stable compound and the deposition temperature is low. A decrease in hardness values with an increase of the deposition temperature could likely be explained by a recovery process leading to a change in a stress-state condition within the composite film/substrate system that affects the response to the indenter penetration process.

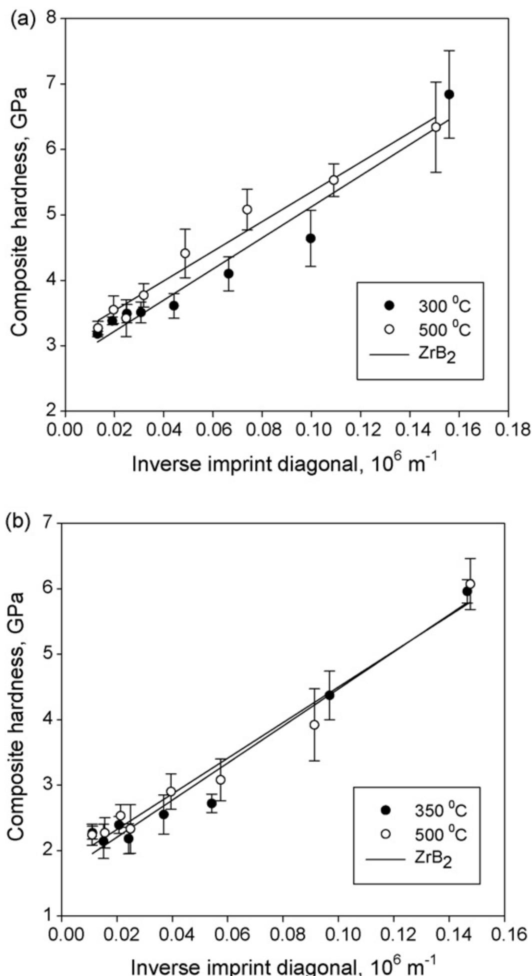

Fig. 5. Composite hardness of film/substrate system versus inverse imprint diagonal: (a) PL-deposited ZrB_2 films on Ti substrate; (b) EB-deposited ZrB_2 on Ti substrate.

A last remark concerns a possible correlation between the hardness of the film and its thickness. Although such correlation can seem theoretically reasonable, the experimental results regarding the films investigated allow to affirm that, even if present, it is negligible within the 0.2–0.5 μm thickness range.

4. Conclusions

(1) Both the PLD and the EBD techniques allowed the deposition of thin compact ZrB_2 films on titanium substrate. The former method enables the deposition of dense crystalline films, grown along the (1 1 0) direction, whereas the electron beam deposition allowed to produce compact amorphous films. The thickness of films was about 200 and 500 nm, respectively.

(2) According to the EDXD rocking curve analysis, the PL-deposited ZrB_2 films are characterized by a preferential (1 1 0) growth. The average size of the (1 1 0) crystallites is (40 ± 5) nm for the PL deposited ZrB_2 films (T_{sp} = 300 °C) and (25 ± 5) nm for the PL deposited ZrB_2 films (T_{sp} = 500 °C). According to SEM analysis, the films surface contains also grains of much larger size (200–250) nm and (250–350) nm, respectively, which is below the detection limit of the EDXD technique.

(3) Vickers hardness of the films was determined from the measured composite hardness of the film-substrate system. The hardness values fall in a range close to that of bulk ZrB_2 ceramics. The results obtained for PL- and EB-deposited ZrB_2 films evidence that, at the same temperature, PL-deposited films are harder. An increase in substrate preheating temperature to 500 °C leads to a decrease in the hardness value of about 22% for PL-deposited samples and of about 17% for EB-deposited ones.

Acknowledgement

The work was supported by a joint CNR (Italian National Research Council)–RAS (Russian Academy of Sciences) project agreement.

References

[1] D. Hertz, H. Michel, T. Belmonte, J.F. Pierson, French Patent FR 2-743-088 (1997).
[2] P. Rogl, P.E. Potter, CALPHAD: Comput. Coupl. Phase Diagr. Thermochem. 12 (2) (1988) 191.
[3] G.V. Samsonov, I.M. Vinitskii, Handbook of Refractory Compounds, IFI/Plenum, 1980.
[4] C.C. Wang, S.A. Akbar, W. Chen, V.D. Patton, J. Mater. Sci. 30 (7) (1995) 1627.
[5] V. Ferrando, C. Tarantini, P. Manfrinetti, I. Pallecchi, M. Salvato, C. Ferdeghini, Thin Solid Films 515 (4) (2006) 1439.
[6] R. Roucka, J. Tolle, A.V.G. Chizmeshya, I.S.T. Tsong, J. Kouvetakis, J. Cryst. Growth 277 (2005) 364.
[7] H. Tamura, M. Konoue, A.B. Sawaoka, J. Thermal Spray Technol. 6 (4) (1997) 463.
[8] J.F. Pierson, T. Belmonte, H. Michel, in: Proceedings of Thirteenth European Conference on Chemical Vapor Deposition, J. Phys. IV 11 (2001) Pr3/85–Pr3/91.
[9] J.F. Pierson, T. Belmonte, T. Czerwiec, D. Hertz, H. Michel, Thin Solid Films 359 (2000) 68.
[10] R. Teghil, A. Giardini Guidoni, A. Mele, S. Piccirillo, M. Coreno, V. Marotta, M. DiPalma, Surf. Interface Anal. 22 (1994) 181.

[11] R. Caminiti, V. Rossi Albertini, Intern. Rev. Phys. Chem. 18 (1999) 263.
[12] D. Ferro, R. Scandurra, A. Latini, J.V. Rau, S.M. Barinov, J. Mater. Sci. 39 (2004) 329.
[13] D. Ferro, J.V. Rau, V. Rossi Albertini, A. Generosi, R. Teghil, S.M. Barinov, Surf. Coat. Technol. 202 (2008) 1455.
[14] B. Jönsson, S. Hogmark, Thin Solid Films 114 (1984) 257.
[15] A. Iost, R. Bigot, Surf. Coat. Technol. 80 (1996) 117.
[16] F. Fröhlich, P. Grau, W. Grellman, Phys. Status Solidi A 42 (1977) 79.
[17] A.M. Korsunsky, M.R. McGurk, S.J. Bull, T.F. Page, Surf. Coat. Technol. 99 (1998) 171.
[18] E.S. Puchi-Cabrera, Surf. Coat. Technol. 160 (2002) 177.
[19] R.W. James, The Optical Principles of the Diffraction of X-rays, Ox-Bow Press, Woodbridge, CT, 1982.
[20] R.A. Andrievski, I.I. Spivak, Strength of Refractory Compounds and Related Materials, Metallurgy, Tcheljabinsk, 1989.
[21] F. Monteverde, A. Bellosi, S. Guicciardi, J. Eur. Ceram. Soc. 22 (2002) 279.